Constructing the Universe with Clusters of Galaxies, IAP 2000 meeting, Paris (France) July 2000
Florence Durret & Daniel Gerbal eds.

DISTANT CLUSTERS: RECENT DETECTIONS IN THE OPTICAL

C. LOBO
CAAUL, Observatório Astronómico de Lisboa
Tapada da Ajuda, 1349-018 Lisboa, Portugal

We have applied a new cluster detection algorithm to the ESO Imaging Survey, thus producing a new catalogue of cluster candidates up to $z \sim 1$. Such a catalogue enables one to perform statistically significant studies as well as detailed research on some of these systems individually and on their member galaxies. The ongoing follow-up of the candidates, in multi-waveband photometry and VLT spectroscopy, is now starting to produce its first results and shall be used later to study the role of environment in the evolution of galaxy populations. Three cluster candidates were thus pre-selected *via* their colors to be observed with FORS1 at the VLT, and the spectra taken turned out to confirm the presence of a system in each field. Redshifts were determined to be z=0.64, 0.66 and 0.71, respectively. Along the line of sight of each candidate, other systems also seem to be present and will be the aim of further research.

1 Introduction

The quest for high–redshift ($z \gtrsim 0.5$) clusters of galaxies has recently received a lot of attention, and several search methods have been put forward and applied to different types of data obtained at different wavelengths.

In fact, the detection and consecutive study of such distant systems has fundamental implications for cosmology (see *eg.* Gioia, this conference) and provides a wealth of knowledge on galaxy evolution.

Thus, optical, near IR, X–ray and even variations in the cosmic microwave background emission are now commonly used to detect cluster candidates at distant redshifts. All different methods have advantages and drawbacks and the key is to view them as complementary.

2 The algorithm and the data set

In this context, and prompted by the ESO Imaging Survey (EIS), we have developed, in a project carried out by Angela Iovino of the Osservatorio Astronomico di Brera (Milano, Italy), myself and other researchers at Milano, a new algorithm[1] to search for distant clusters of galaxies on catalogues deriving from optical imaging data.

Table 1: Limits of the regions to be analyzed by our algorithm (coordinates are expressed in equinox J2000).

patch	α_{min} $(h\ m\ s)$	α_{max} $(h\ m\ s)$	δ_{min} $(^o\ '\ ")$	δ_{max} $(^o\ '\ ")$
A	22 35 31	22 49 41	-40 28 37	-39 27 36
B	00 44 30	00 54 01	-29 53 24	-29 17 24

2.1 Overview of the EIS-wide and derived catalogues

The EIS-wide[2], covering a final area of 17 square degrees of the southern sky in the I-band, up to limiting magnitude $I \sim 23$, provided us with the catalogues[3] of object positions and magnitudes in a double coverage (henceforth referred to as the even and the odd) of each region of the survey.

We worked on patches A and B of the survey, limiting the data set to $18 \leq I \leq 22.0$ and extracting the galaxy catalogue - on which we would run our algorithm - according to a careful star-galaxy separation.

For technical reasons, we trimmed each patch so as to have clear-cut rectangular edges. This translates into the limits given in table 1, and in the following numbers of galaxies: 57366 for patch A–even, 57553 for patch A–odd, 25456 for patch B–even and 25445 for patch B–odd. In summary, we have four catalogues, two (the even and the odd) for each patch, where we shall independently run our algorithm.

We also note that the adopted limits for each patch are such that our analysis covers surfaces that total, respectively, around 3 square degrees in the case of patch A and 1.4 square degrees for patch B.

2.2 The new algorithm

In their pioneering work[4] on the Palomar Distant Cluster Survey, Postman and collaborators (P96 hereafter) wrote a matched filter algorithm to identify cluster candidates by using positional and photometric data simultaneously. Our work tries to improve on the P96 algorithm in the sense of removing the *a priori* assumptions that are implicit in the P96 technique and of optimizing the suitability of the algorithm to the characteristics of the data set we are dealing with in particular.

The P96 algorithm relies on the choice of both a given cluster profile - modified–Hubble or King–like - with a typical cluster scale - the core radius r_c - and a cut–off radius, and of a typical M^* - the chosen parameterization of the Schechter function. Both quantities, r_c and M^*, are rigidly coupled to detect cluster candidates and assign them a tentative redshift. Each one of these quantities being a function of distance (and thus cosmology), their implementation on any algorithm implies a dependence on the adopted cosmology and on the chosen amount of evolution, not to mention the dependence on the particular values actually chosen for r_c and M^*.

In our new algorithm the spatial and luminosity part of the filter are run separately and successively on the catalogue, with no assumption on the typical size or typical M^* for clusters. In fact, these parameters intervene in our algorithm only as a typical angular scale and typical apparent magnitude m^*, bearing no ties to fixed physical scales nor to absolute magnitudes through redshift dependence. This has the consequence of removing the need for a choice of fixed physical values for these two quantities, and for a choice of evolutionary models. Moreover, the fact of not coupling the space and the luminosity parameters also enables us to reach higher values of completeness: a candidate can be retrieved even if it does not flag a maximum likelihood

at the very same redshift value simultaneously for both the space and the luminosity distributions (a situation that would lower its global likelihood when using the P96 algorithm).

We also perform a local estimate of the background for each cluster candidate, which allows us to tackle the problems of inhomogeneities in the EIS data that may hamper the detection in shallower regions of the catalogue which are actually present due to reported[5] varying observing conditions, at least in part of the EIS data.

In our algorithm, local enhancements in the projected galaxy density are first selected through a Gaussian filtering, where we use five different angular sizes σ_{ang}, namely from ~ 0.35 up to ~ 1.42 arcmin in five steps of ratio $\sqrt{2}$. These values were chosen bearing in mind the range of reasonable dimensions of the cluster candidates spanning the redshift interval that we expected to probe with the EIS data ($z \lesssim 1.2$). A simple cross-correlation at the end of this step allows us to remove multiple detections of the same candidate obtained with different filter widths.

To conclude the spatial filtering, a "spatial probability" of a candidate being spurious is computed.

Subsequently, a maximum-likelihood "filtering" on the apparent magnitudes searches for the presence of a Schechter[6] distribution superimposed on the local background (which follows a power–law instead). Unlike P96, we have decided to implement the generalized treatment[7] for this likelihood filter, thus using the exact mathematical equations, which does not add major computational effort nor time. Besides, it also renders unnecessary the final *"cluster signal correction"* demanded by the complex approximations of the P96 procedure.

The only parameter that we fix for the Schechter function is the slope of the faint end, $\alpha = -1.25$, according to the observational value determined[8] for a set of 14 clusters at mean redshift $< z > \simeq 0.0851$.

This second step of the algorithm leads to the assessment of a corresponding "luminosity probability" that, multiplied by the spatial one, produces the final probability of each candidate being a spurious one. This means that the lower this value, the more confident the candidate. Notice also that this final quantity is always lower than either one of the partial spatial or luminosity probabilities as it is their product. We note that we shall often interchange probability with the complementary Gaussian percentile and the associated level of standard deviations, referred to as S/N throughout this paper. This approximation was used also in P96 so, by adopting it as well, we render comparisons among our results easier.

2.3 Selection of the candidates

If we had two good quality even and odd catalogues for each patch, we could just apply a cut–off on both catalogues and get two final lists of cluster candidates that should differ by a small number, caused by false detections in regions where spurious objects had been detected[3] (by SExtractor) in the spikes of bright saturated stars or satellite tracks.

Unluckily, this does not appear to be the case for the data, especially in what concerns patch A, whose CCD frame quality is quite variable[5]. As a result, applying a blind cut–off to both catalogues would be too restrictive a choice, and therefore we decided to follow a more flexible approach, described next.

For each patch we first built, for the corresponding even and odd galaxy catalogue, a catalogue of cluster candidates with a S/N cut–off of 3. Then, from these catalogues we selected:

> *Class 1* candidates: present in both even and odd catalogues (which implicitly means that they have $S/N \geq 3.0\sigma$ in both catalogues) with $S/N \geq 4.0\sigma$ in at least one of them;

Class 2 candidates: present in one catalogue only but having $S/N \geq 4.0\sigma$.

In terms of contamination, our choice is equivalent to applying a $S/N \geq 4.0$ cut–off to the even/odd catalogues separately and the same holds for completeness, but with the further constraint for *class 1* candidates of being present also in the odd/even catalogue with $S/N \geq 3.0$ (no further constraint for *class 2* candidates).

In section 2.4 we will show that a cut–off value of $S/N = 4\sigma$ gives a low number of contaminants of ~ 1.3 per square degree, while guaranteeing a high level of completeness for a significant range of cluster richness classes.

2.4 Algorithm performance

Extensive bootstrap simulations of mock catalogues (obtained by random shuffling galaxy positions and magnitudes of the EIS galaxy catalogues built in section 2.1) were submitted to the algorithm, thus allowing us to estimate an expected contamination rate of 1.3 false candidates per square degree for the adopted $S/N = 4\sigma$ threshold.

As for completeness, we added realistic cluster galaxies to the mock catalogues and computed the rate of recovery of these systems by the algorithm. The clusters span the Abell richness classes $R = 1$ (poor), $R = 2$ (intermediate) and $R = 3$ (rich), and have a power law radial profile of type $r^{-1.4}$. They are dominated by ellipticals, and have a typical luminosity function[8]. We applied elliptical k-corrections[9] to the member galaxies.

Results are shown in figure 1.

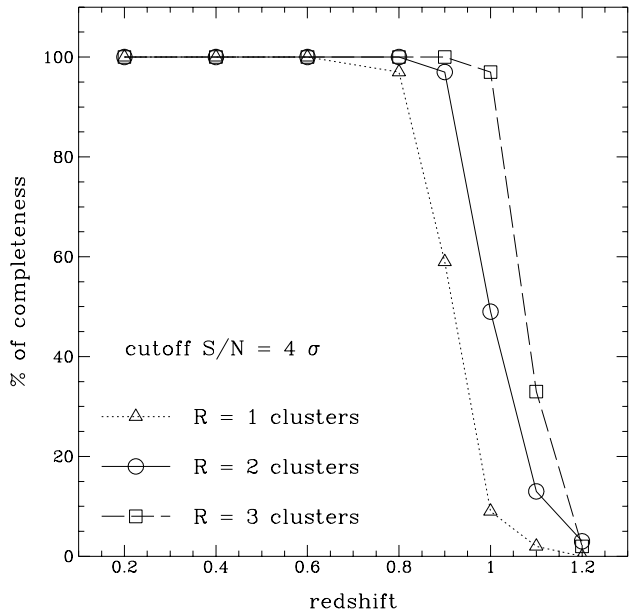

Figure 1: Percentage of completeness for different Abell richness class clusters as established through simulations.

3 The cluster candidates

Our final catalogues contain the following entries for each one of the candidate clusters found in the EIS-wide patches A and B: right ascension and declination (equinox 2000), indicative

angular size (proportional to σ_{ang}), combined total probability expressed as a S/N, m^*, redshift and richness estimates.

The last two quantities are not direct products of our algorithm, unlike what happens when using the P96 method. We thus have to estimate them *a posteriori*. In what concerns the redshift, we can assess it by using m^* and its relationship to M^*, whose adopted value is that reported by observations[8], to be redshifted and corrected using the k-corrections typical of ellipticals[9].

In fact, the simulations (that allowed us to assess the overall completeness rate - see section 2.4) show that the value of m^* obtained with our algorithm retrieves well the M^* introduced in the simulations - see figure 2.

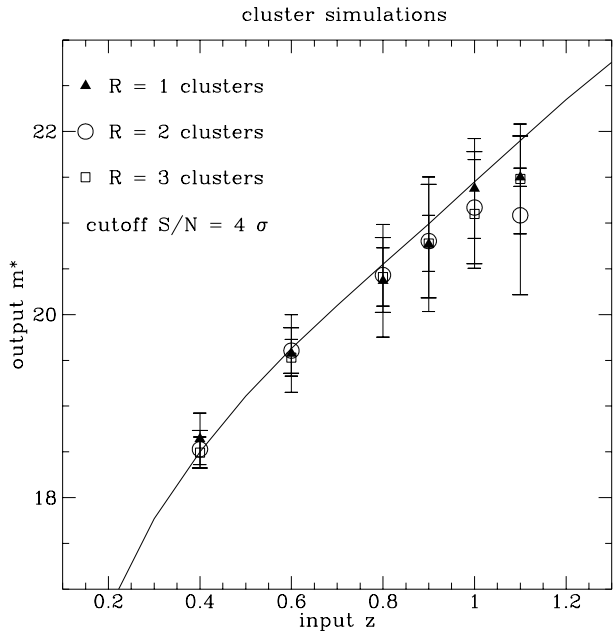

Figure 2: Results from the simulations showing the comparison between the redshift value of the simulated clusters and the output m^* obtained from our algorithm. The curve shows the relationship between z and m^* used to define the input m^* in our simulations. Each point is the mean of 100 simulations. 1σ error bars are drawn.

Once we have an idea of the cluster candidate's redshift, we can produce an estimate for its richness. We chose to do so through the estimator proposed by Bahcall (1981), $N_{0.5}$. It consists in counting the number of cluster member galaxies brighter than $m_3 + 2$ (where m_3 is the magnitude of the third brightest cluster galaxy), located within a projected radius of 0.5 Mpc from the cluster center[a]. Background correction is estimated from similar counts performed in the entire catalogue region, using 0.2 magnitude bins. The $N_{0.5}$ parameter has already been used in the literature for richness estimates of distant clusters[11].

$N_{0.5}$ can be translated into the typical Abell richness classes using an indicative relation[10], $N_{Abell} \simeq 3.3 \times N_{0.5}$, and knowing that $N_{0.5} < 15$ corresponds[12] to Abell richness class $R \sim 0$, while $N_{0.5} > 24$ is equivalent to $R \gtrsim 2$.

The final distribution of our *class 1* and *class 2* candidates in the two patches can be seen in figure 3.

The redshift and richness distributions of the candidates are given in figures 4 and 5. Note that the median of the redshift distribution for *class 1* candidates, patch A and B considered

[a] We adopt $H_0 = 50$ km s^{-1}Mpc^{-1} and $q_0 = 0.5$ throughout this paper.

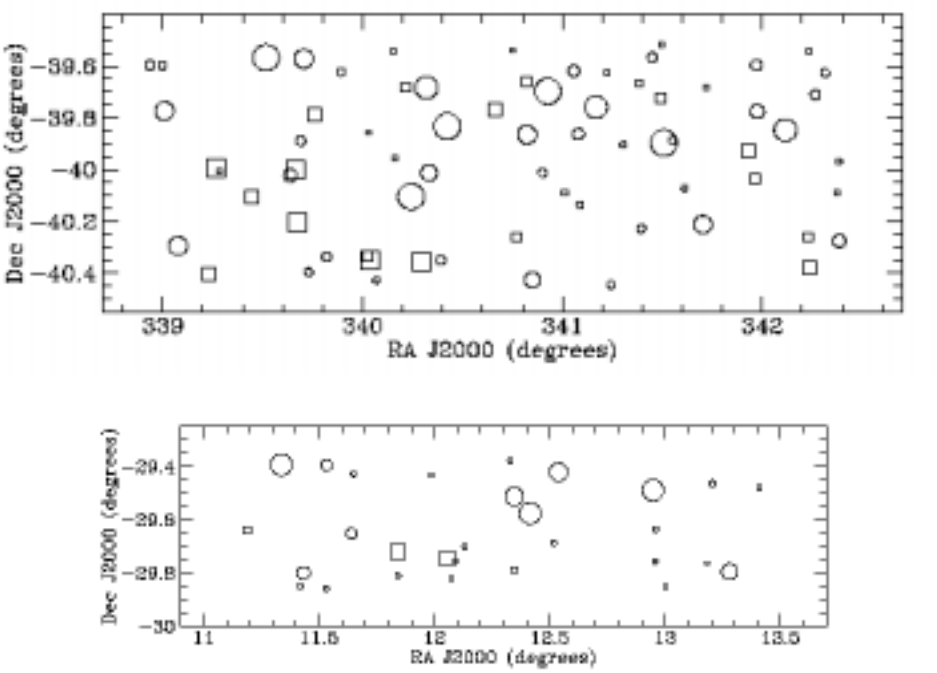

Figure 3: Map of patch A candidates (upper panel) and patch B ones (lower panel). Circles indicate *class 1* systems while squares designate *class 2* candidates. The total number of detections, both *classes* considered together, is of 70 in patch A and 29 in patch B. Coordinates and sizes (proportional to σ_{ang}) are mean values from even and odd catalogues.

together, is $z = 0.65$.

A detailed comparison between our catalogues of cluster candidates and those of the EIS-team[13 5] has been thoroughly made[1], while we also checked[1] the matching of our candidates with those proposed by previous independent works and listed in the NED database.

4 Perspectives

We have undertaken a campaign to do multi-waveband photometry for all our cluster candidates. The aim is to clean our catalogues from residual spurious detections and to prepare the spectroscopic follow-up of a handful of the most promising systems.

4.1 Photometric follow-up

These observations were designed so as to give us a good compromise which would allow us to reach simultaneously as deep (in fractions of L_*) and as wide (in cluster radial extent) and as distant (in redshift) as previous works manage only for one (mostly two) of these parameters at a time.

We have been using the 3.6-m and NTT ESO telescopes which imaging cameras (EFOSC2 and SUSI2) provide a good sampling surface (of about 5.5 arcmin $\times$ 5.5 arcmin) of the cluster candidates. We thus cover them approximately up to the cluster virial radius, for which 2 arcmin is a good estimate in the case of a typical rich cluster at $z \sim 0.6$.

These observations allow us to get a handle on cluster members through color selection (which will also be useful to determine slit positions for spectroscopic follow-up), compute photometric redshifts and, eventually if data quality allows, produce an indication of morphologies[14] and perform some analysis of the entropy of cluster member galaxies as a secondary distance

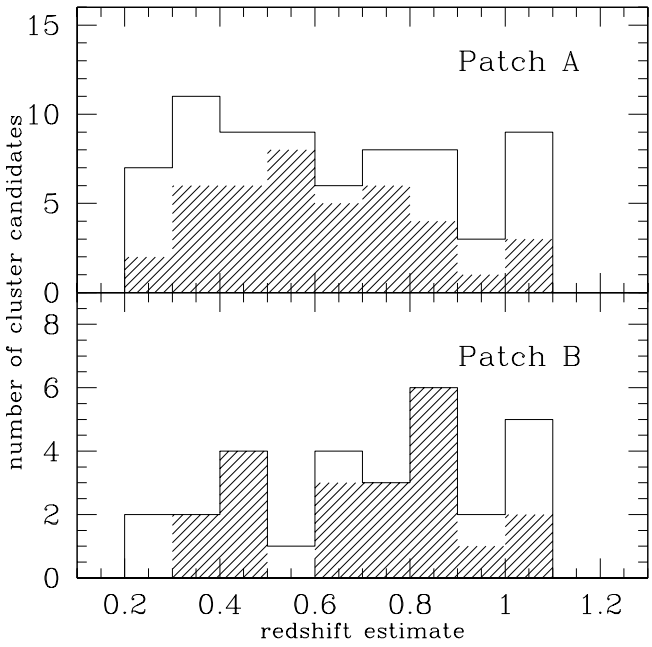

Figure 4: Redshift distribution for the cluster candidates flagged in patch A - upper panel - and patch B - lower panel. Hatched histograms specify matched (*class*1) detections among the global distribution (empty histograms). In this figure the z plotted for each cluster candidate is the mean value obtained from even and odd catalogues.

indicator (see the paper presented by I. Márquez in this conference).

The combined color images of our most striking cluster candidates can be seen at:
http://www.oal.ul.pt/∼lobo/EIScls.html

4.2 Spectroscopic follow-up

Two nights of FORS spectroscopy were carried out at the VLT UT1 to get spectra for three of our cluster candidates. These had been selected *via* their colors as potential distant systems, placed at $z > 0.5$.

In fact, the results from these observations turned out to confirm the presence of a system in each field. Redshifts were determined to be z=0.64, 0.66 and 0.71, respectively. Along the line of sight of each candidate, other systems, including a group of actively star forming galaxies at z=0.25, also seem to be present and will be the aim of further research. Serote Roos, in this same conference, reports some of these results.

We will hopefully re-observe these clusters in order to reach a significant coverage of the cluster members in spectroscopy, so as to allow us to make detailed studies on these systems. Some of our goals are to determine their luminosity functions, get an idea of their dynamical mass and structural properties and, if data allows, perform a spectral population synthesis analysis and fundamental plane researches.

Acknowledgments

It is a pleasure to thank my collaborators, in particular D. Lazzati, whose work was essential to write the cluster detection algorithm. L. Guzzo is warmly thanked for discussions and comments. I acknowledge financial support by the CNAA fellowship reference D.D. n.37 08/10/1997, and also the FCT PRAXIS XXI fellowship BPD/20174/99, and the ESO/PRO/15130/1999 project.

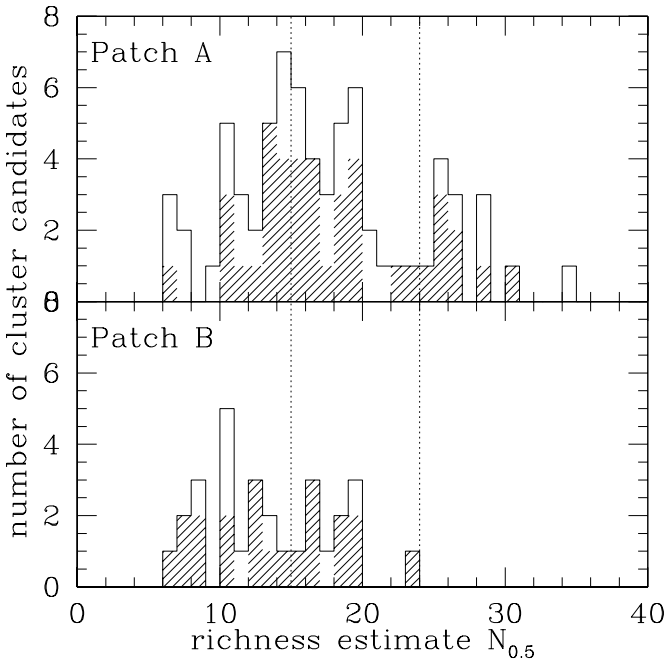

Figure 5: Distribution of the richness estimate $N_{0.5}$ for the cluster candidates flagged in patch A - upper panel - and patch B - lower panel. Hatched histograms specify matched detections among the global distribution (empty histograms). The dotted lines mark the approximate limits between Abell richness classes 0 and 1 (at $N_{0.5} \sim 15$) and Abell richness classes 1 and 2 ($N_{0.5} \sim 24$). The $N_{0.5}$ plotted for each cluster candidate is the mean value obtained from even and odd catalogues.

References

1. C. Lobo, A. Iovino, D. Lazzati, G. Chincarini, astro-ph/0006431.
2. A. Renzini & L. da Costa, *The Messenger* **87**, 23 (1997).
3. M. Nonino, E. Bertin, L. da Costa *et al.*, *A&AS* **137**, 51 (1999).
4. M. Postman, L.M. Lubin, J.E. Gunn *et al.*, *AJ* **111**, 615 (1996).
5. L.F. Olsen, M. Scodeggio, L. da Costa *et al.*, *A&A* **345**, 681 (1999b).
6. P. Schechter, *ApJ* **203**, 297 (1976).
7. P. Schuecker & H. Böhringer, *A&A* **339**, 315 (1998).
8. M. Colless, *MNRS* **237**, 799 (1989).
9. M. Fioc & B. Rocca-Volmerange, *A&A* **326**, 950 (1997).
10. N. Bahcall, ApJ **247**, 787 (1981).
11. J.–M. Deltorn, O. Le Fèvre, D. Crampton, M. Dickinson, ApJ **483**, L21 (1997).
12. N. Bahcall, ARAA **26**, 631 (1988).
13. L.F. Olsen, M. Scodeggio, L. da Costa *et al.*, *A&A* **345**, 363 (1999a).
14. R.G. Abraham, F. Valdes, H.K.C. Yee, S. van den Bergh, ApJ **432**, 75 (1994).